Expression of Frzb/Secreted Frizzled-Related Protein 3, a Secreted Wnt Antagonist, in Human Androgen-Independent Prostate Cancer PC-3 Cells Suppresses Tumor Growth and Cellular Invasiveness

Xiaolin Zi,[1] Yi Guo,[2] Anne R. Simoneau,[1] Christopher Hope,[3] Jun Xie,[2] Randall F. Holcombe,[3] and Bang H. Hoang[2]

Departments of [1]Urology, [2]Orthopaedic Surgery, and [3]Medicine and Chao Family Comprehensive Cancer Center, University of California, Irvine, Orange, California

Abstract

The ability of Frzb/secreted Frizzled-related protein 3 (sFRP3) to inhibit Wnt signaling and the localization of Frzb/sFRP3 on chromosome 2q to a region frequently deleted in cancers have led some investigators to hypothesize that Frzb/sFRP3 is a tumor suppressor gene. Here, we examined the biological effects of Frzb/sFRP3 on an androgen-independent prostate cancer cell model. We showed that expression of Frzb/sFRP3 in PC-3 cells resulted in decreased colony formation in soft agar and a dramatic inhibition of tumor growth in a xenograft mouse model. When cellular morphology was examined, PC-3 cells expressing Frzb/sFRP3 exhibited an increase in cell-cell contact formation accompanied by a pronounced induction of epithelial markers E-cadherin and keratin-8 and down-regulation of mesenchymal markers N-cadherin, fibronectin, and vimentin. This phenomenon suggested a reversal of epithelial-to-mesenchymal transition and a less invasive phenotype. Indeed, further *in vitro* studies with a Matrigel assay showed that Frzb/sFRP3 decreased the invasive capacity of PC-3 cells. These changes in the biology of PC-3 cells are associated with a decrease in the expression and activities of both matrix metalloproteinase (MMP)-2 and MMP-9 as well as decreases in AKT activation, cytosolic β-catenin levels, T-cell factor transcription activity, and expression of Slug and Twist. In addition, transfection of PC-3 with a dominant-negative low-density lipoprotein receptor–related protein 5 (DN-LRP5) coreceptor showed similar biological effects as Frzb/sFRP3 transfection. Together, these data suggest that Frzb/sFRP3 and DN-LRP5 exhibit antitumor activity through the reversal of epithelial-to-mesenchymal transition and inhibition of MMP activities in a subset of prostate cancer. (Cancer Res 2005; 65(21): 9762-70)

Introduction

Understanding the biological basis of cancer is one of the most effective methods for developing safe and effective prevention and treatment strategies. Given that each prostate cancer diagnostic type represents a heterogeneous group of lesions (1), multiple growth and survival characteristics likely contribute to the carcinogenesis and neoplastic progression of this disease. Activation of the Wnt/β-catenin pathway has been observed in a portion of prostate cancer patients (2, 3), and this pathway has been shown to modulate androgen action in the prostate (4, 5), implying that alterations in Wnt signaling may influence prostate tumor biology.

Wnts, a family of secreted cysteine-rich glycoproteins, act as ligands to activate Frizzled receptor–mediated signaling pathways (6). During normal development, cells respond to Wnts in a context-dependent fashion by undergoing changes in cell proliferation, patterning, fate determination, and movement (6). In adults, aberrant activation of Wnt signaling has been reported to be involved in tumorigenesis (6). Wnt ligands seem to activate one or more intracellular signaling pathways depending on the type of ligands, Frizzled receptors, and cells (6). The best-studied Wnt signaling pathway is the Wnt/β-catenin pathway, in which Wnt ligands form a complex with Frizzled receptor and coreceptor low-density lipoprotein receptor–related protein 5 (LRP5) or LRP6 (6, 7). Receptor activation inhibits the adenomatous polyposis coli-Axin "destruction complex," where β-catenin is phosphorylated by both casein kinase I and glycogen synthase kinase-3β (GSK-3β) and targeted for ubiquitination by βTrCP or Siah leading to degradation in the 26S proteosome (7). This inhibition results in cytoplasmic β-catenin stabilization and facilitates its translocation into the nucleus (6, 7). In the nucleus, β-catenin relieves inhibition of transcription factors T-cell factor (TCF)/lymphoid enhancer factor (LEF) by repressors leading to transcription of target genes, such as *c-myc, matrix metalloproteinase* (*MMP*)*-7, cyclin D1*, etc. (6, 7). In addition, Wnts can activate β-catenin-independent pathways leading to changes in cell movement and polarity (8).

Secreted Wnt antagonists, classified as secreted Frizzled-related protein (sFRP) family, Dickkopf family, and Wnt inhibitory factor-1, are potential negative modulators of Wnt signaling (9). The sFRPs contain a cysteine-rich domain (CRD), highly homologous to the extracellular, ligand-binding domain of Frizzled receptors (9). sFRPs have been shown to inhibit Wnt signaling either by sequestering Wnt ligands or by forming nonfunctional complexes with Frizzled receptors (9). Recently, down-regulation of sFRPs by gene deletion or promoter hypermethylation has been shown in many human cancers (10–15).

Frzb/sFRP3, the first member of the sFRP family, was isolated as a chondrogenic factor in developing cartilage (16). Frzb/sFRP3 binds to both Wnt-8 and Wnt-1 and acts as a functional inhibitor of Wnt-8 activity in *Xenopus* embryos (17, 18). Human Frzb/sFRP3 has been recently mapped to human chromosome 2q31-33 (19). Deletions of chromosome 2q occur in prostate carcinoma (20, 21).

Note: Supplementary data for this article are available at Cancer Research Online (http://cancerres.aacrjournals.org/).

Requests for reprints: Xiaolin Zi or Bang H. Hoang, Department of Urology and Chao Family Comprehensive Cancer Center, Room 431, Building 23, Route 81, 101 The City Drive South, Orange, CA 92868. Phone: 714-456-8316; Fax: 714-456-2240; E-mail: xzi@uci.edu.

doi:10.1158/0008-5472.CAN-05-0103

One study reported loss of heterozygosity at 2q32-q36 in 42% (6 of 14) of prostate carcinomas (21). Allelic loss at chromosome 2q has been observed at high frequency in advanced disease in contrast to much lower rates in early-stage tumor specimens from patients with gastric cancer (22), papillary bladder cancer (23), and non–small cell lung carcinoma (24). Moreover, mortality in patients with head and neck cancer was reported to strongly correlate with loss of heterozygosity on chromosome 2q (25). These data suggest that inactivation of one or more tumor suppressors on chromosome 2q may result in aggressive behavior of various human malignancies. Given the oncogenic properties of certain Wnts and the frequent loss of chromosome 2q in human cancers, Frzb/sFRP3 has been hypothesized by some investigators to act as a tumor suppressor (17–19). Here, we examined the biological effects of Frzb/sFRP3 on prostate cancer using an androgen-independent cellular model. Ectopic expression of Frzb/sFRP3 in PC-3 cells resulted in inhibition of colony formation and loss of tumorigenicity in nude mice as well as a decrease in cellular invasiveness. These effects of Frzb/sFRP3 are associated with a dramatic induction of E-cadherin and keratin-8, down-regulation of N-cadherin, fibronectin, and vimentin, and inhibition of the activities and expression of both MMP-2 and MMP-9.

Materials and Methods

Cell culture, plasmid, and stable transfection. PC-3, 22RV1, LNCaP, and DU145 cells were obtained from American Type Culture Collection (Manassas, VA) and maintained in RPMI supplemented with 10% fetal bovine serum (FBS) and antibiotics. Primary prostate epithelial cells came from Cambrex Bioscience (Walkersville, MD) and were grown in prostate epithelial basal medium. The *PCDNA3.1*, containing a full-length 2.4-kb *Bam*HI-*Xho*I fragment of bovine *Frzb/sFRP3*, was a generous gift of Frank P. Luyten (Universitaire Ziekenhuizen, Leuven, Belgium). *Dominant-negative (DN) LRP5* was a generous gift of Dr. Matthew Warman (Case Western Reserve University, Cleveland, OH). *DN-TCF4* was from Dr. T.C. He (University of Chicago Medical Center, Chicago, IL). *DN-LRP5* is a secreted form of LRP5 that lacks the transmembrane and cytoplasmic domains (δTM; ref. 26). *Frzb/sFRP3* and *DN-TCF4* were described previously in detail (16, 27). The *LEF1* expression construct FL9B, the *TCF4* luciferase reporter (TOPFLASH), and a mutated control reporter (FOPFLASH) were from Dr. Marian Waterman (University of California, Irvine, CA). *DN-LEF1* was constructed as follows: A neomycin/kanamycin resistance expression cassette was PCR amplified from pCMV-Script using primers 5′-CACCC-GGTGCACTTAATGCGCCGC-3′ and 5′-AGTTCGGTGTAGGTCGTTCG-3′. The product was restriction digested with *Apa*LI and cloned into an *Apa*LI-digested FL9B to generate the FL9B-Neo construct. Oligonucleotides 5′-GATCCAACGGACACGAG-3′ and 5′-GTGTCCGTTG-3′ were annealed and ligated into *Dra*III/*Bam*HI–digested FL9B-Neo to generate the *DN-LEF1* construct used in these studies. For stable transfection, PC-3 cells were plated at 1×10^6 per 100-mm dish. At 60% confluency, cultures were transfected with *PCDNA3.1, Frzb/sFRP3, DN-LRP5, DN-LEF1*, or *DN-TCF4* using FuGENE 6 (Roche, Indianapolis, IN). Transfected cells were selected with G418 (800 μg/mL) starting at 48 hours after transfection, and all of the stable transfectants were pooled to avoid cloning artifacts. Pooled stable clones of PC-3 cells expressing Frzb/sFRP3, DN-LRP5, DN-TCF4, DN-LEF1, or PCDNA3.1 were maintained in RPMI containing 10% FBS and 500 μg/mL G418.

Luciferase and β-galactosidase assays. PC-3 cells stably expressing PCDNA3.1, Frzb, or DN-LRP5 were grown in six-well plates and transiently cotransfected with 1 μg pTOPFLASH or pFOPFLASH and 0.1 μg *cytomegalovirus (CMV)-β-galactosidase* plasmids (Invitrogen, Carlsbad, CA) using FuGENE 6. After 24 hours of incubation, cells were harvested and the luciferase and β-galactosidase activities were measured using Bright-Glo luciferase assay system and β-galactosidase enzyme assay system (Promega, Madison, WI). The relative luciferase unit for each transfection was adjusted by β-galactosidase activity in the same sample.

Protein extraction, conditioned medium, and Western blotting. For extraction of membrane and cytosolic proteins (28), cells were collected in TES suspension buffer and homogenized on ice. The cytosolic fraction was recovered by ultracentrifugation at 100,000 × *g*. The membrane-enriched pellet was solubilized in solubilization buffer. For extraction of total proteins, cells were lysed in radioimmunoprecipitation assay buffer. Conditioned media were prepared using serum-free RPMI by culturing PC-3 cells stably transfected with vector control, *Frzb/sFRP3*, or *DN-LRP5* at 70% confluence for 48 hours and concentrated 40 times by Centricon (Millipore, Bedford, MA). Clarified protein lysates (20-80 μg) or concentrated conditioned medium was electrophoretically resolved on denaturing SDS-polyacrylamide gel (8-16%), transferred to nitrocellulose membranes, and probed with antibodies against β-catenin (Upstate Biotechnology, Charlottesville, VA), E-cadherin, P-cadherin, and N-cadherin (BD Biosciences, San Diego, CA), keratin-8, keratin-18, fibronectin, and vimentin (Lab Vision, Fremont, CA), GSK-3β and phospho-GSK-3β (Cell Signaling, Beverly, MA), LRP5 (Orbigen, San Diego, CA), c-myc (Calbiochem, San Diego, CA), cyclin D1, Slug, Twist, FRP3 (sFRP3/Frzb), and β-actin (loading control; Santa Cruz Biotechnology, Santa Cruz, CA). Proteins were revealed using secondary antibodies and visualized by an enhanced chemiluminescence detection system (Amersham Bioscience, Piscataway, NJ).

Immunocytofluorescence assay. Cells were cultured in chamber slides (Lab-Tek). After methanol fixation and permeabilization with Triton X-100, cells were incubated with an anti–E-cadherin antibody (BD Biosciences), an anti-FLAG antibody (Invitrogen), or an anti-MYC antibody (Cell Signaling) and then with an Alexa 488–conjugated secondary antibody (Molecular Probes, Inc., Eugene, OR). Localizations of E-cadherin, FLAG-tagged Frzb/sFRP3, MYC-tagged DN-LRP5, and DN-TCF4 were analyzed under confocal microscopy (Zeiss, Thornwood, NY) using the 488 nm excitation wavelengths of the laser.

Real-time PCR. RNA isolation and real-time PCR methods were described in Supplementary Fig. S1A legend. Real-time PCR for quantitation of the mRNA levels of *E-cadherin, Twist*, and *Slug* was done using a Bio-Rad MyiQ thermocycler (Bio-Rad, Hercules, CA) and primer sets listed in Supplementary Table S1. Data were analyzed by using the comparative C_t method (29), where C_t is the cycle number at which fluorescence first exceeds the threshold. The C_t values from each sample were obtained by subtracting the values for *β-actin* C_t from the *E-cadherin, Twist*, or *Slug* C_t value. The variation of *β-actin* C_t values is <0.5 among different samples. One difference of C_t value represents a 2-fold difference in the level of mRNA. Specificity of resulting PCR products was confirmed by melting curves.

Matrigel invasion assay. To assay cell motility, 2.5×10^4 cells per well in serum-free RPMI were placed in the upper chamber. RPMI plus 10% FBS was placed in the lower chamber as a source of chemoattractant. Cells were allowed to migrate through a porous, uncoated membrane (BD Biosciences) for 24 hours at 37°C. Nonmigratory cells in the upper chamber then were removed with a cotton-tip applicator. Migrated cells on the lower surface were fixed with methanol and stained with hematoxylin. The number of migrating cells was determined by counting 10 high-power fields (×100) on each membrane and calculated as mean number of cells per field. For invasion assays, 24-well invasion chamber system (BD Biosciences) was used. Viable cells (2.5×10^4/well) in serum-free RPMI were seeded in the upper chamber coated with Matrigel. RPMI plus 10% FBS was placed in the bottom well. Incubation was carried out for 48 hours at 37°C. The membrane was processed as described for the motility assay. An invasion index, corrected for cell motility, was calculated as follows:

$$\frac{\text{No. of cells invaded through a Matrigel} - \text{coated membrane}}{\text{No. of cells migrated through an uncoated (control) membrane}} \times 100$$

All of the cell lines were assayed in triplicate for each experiment, and each experiment was repeated thrice.

Gelatin zymography. Samples were applied to nondenaturing 10% polyacrylamide gels containing 1 mg/mL gelatin. After electrophoresis, the gels were washed with 2.5% Triton X-100, incubated overnight at 37°C in zymography buffer, and stained with Coomassie brilliant blue. Gelatinolytic activity was visualized as clear areas of lysis in the gel.

Soft agar colony formation. A soft agar colony formation assay was done using six-well plates. Each well contained 2 mL of 0.5% agar in complete medium as the bottom layer, 1 mL of 0.38% agar in complete medium and 3,000 cells as the feeder layer, and 1 mL complete medium as the top layer. Cultures were maintained under standard culture conditions. The number of colonies was determined with an inverted phase-contrast microscope at ×100 magnification; a group of >10 cells was counted as a colony. The data are means ± SE of four independent wells at optimum time of 14 days after the start of cell seeding.

***In vivo* tumor model.** NCR-*nu/nu* (nude) mice were obtained from Taconic (Germantown, NY). Cells from each stable line were concentrated to 2×10^6 per 200 μL and injected s.c. into the left flank of each mouse. Once xenografts became established, their sizes were measured every 4 days. The tumor volume was calculated by the formula: $0.5236L_1(L_2)^2$, where L_1 is the long axis and L_2 is the short axis of the tumor. All of the animal studies were approved by the Institutional Animal Care and Use Committee at University of California (Irvine, CA).

Statistics. Comparisons of cell density, number of colonies, invasion index, relative levels of mRNA expression, and relative levels of protein expression between the different transfections were conducted using Student's *t* test. For tumor growth experiments, repeated-measures ANOVA was used to examine the differences in tumor sizes among different transfections, time points, and transfection-time interactions. Additional post-test was done to examine the differences in tumor sizes between vector control and other transfections at each time point by using conservative Bonferroni method. All statistical tests were two sided. $P < 0.05$ was considered statistically significant.

Results

Frzb/secreted Frizzled-related protein 3 specifically decreases anchorage-independent growth and increases anchorage-dependent growth of PC-3 cells. Compared with other prostate epithelial cell lines, the expression of the LRP5 coreceptor (required for canonical Wnt signaling) was significantly up-regulated in PC-3 cells (Fig. 1*A, top*). In addition, Frzb/sFRP3 protein expression was detected as a doublet only in the normal prostate epithelial cell line (PrEC) but absent in prostate cancer cell lines (22RV1, LNCaP, DU145, and PC-3). This doublet band of Frzb/sFRP3 may be a result of glycosylation (16, 17). As shown by real-time PCR, PC-3 cells also lack expression of several other secreted Wnt antagonists (Supplementary Fig. S1A). In a microarray data set generated by Dhanasekaran et al. (30), down-regulation of *Frzb* mRNA (cDNA clone IMAGE:140071, *Frizzled-related protein*) was found in bone metastatic prostate cancer specimens compared with commercial prostate reference pool, benign prostatic hyperplasia, and prostatitis. Together, these data lead us to select PC-3 cells (derived from bone metastatic prostate cancer) as a model to examine the biological effects of Frzb/sFRP3 or disruption of LRP5-mediated signaling on prostate cancer.

We stably transfected PC-3 cells with either Frzb/sFRP3 or DN-LRP5 or PCDNA3.1 control vectors. The expression of Frzb/sFRP3 or DN-LRP5 in stable clones was confirmed by Western blot analysis of FLAG and MYC tag protein in both conditioned medium and cell lysates (Fig. 1*B*). The concentration of Frzb/sFRP3 in the conditioned medium was estimated to be ~15 ng/mL (by comparison with known concentration of recombinant sFRP3). Immunocytofluorescence staining of Frzb/sFRP3 transfected cells showed that Frzb/sFRP3 was localized in the membrane and cytoplasm (Supplementary Fig. S1B). By immunocytofluorescence, we estimated the expression of *Frzb, DN-LRP5*, and *DN-TCF4* transgenes to be ~70% to 80% positive (data not shown). We were unable to estimate the percentage expression of *DN-LEF1* transgene due to lack of a tag protein in this construct.

Figure 1*C* and *D* showed that expression of Frzb/sFRP3 inhibited the anchorage-independent growth of PC-3 cells. For control transfectants, 63 ± 3.5 (mean ± SE of four wells) colonies

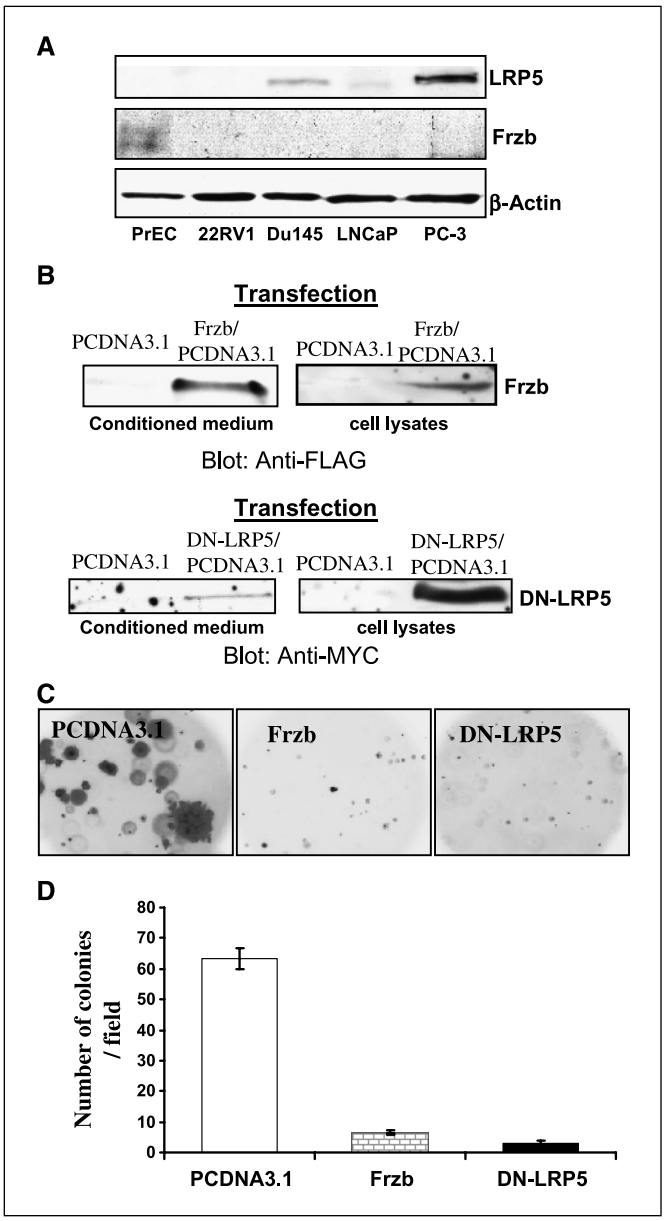

Figure 1. Ectopic expression of Frzb/sFRP3 and DN-LRP5 in PC-3 cells decreases anchorage-independent growth. *A,* protein expression of human LRP5 and Frzb/sFRP3 in normal prostate epithelial cells and prostate cancer cell lines. *B,* Frzb and DN-LRP5 expressions in the conditioned medium and cell lysates of the transfectants were determined by Western blotting with anti-FLAG and anti-MYC, respectively. *C,* qualitative analysis of soft agar colony formation in PC-3 cells expressing PCDNA3.1 vector control, Frzb, or DN-LRP5. Representative photographs from four independent experiments taken under an inverted phase-contrast microscope at ×100 magnification. *D,* quantitative analysis of soft agar colony formation of PC-3 cells expressing PCDNA3.1 vector control, Frzb, or DN-LRP5. *Columns,* mean of four independent wells at optimum time of 14 days after the start of cell seeding; *bars,* SE.

per field were counted compared with seven colonies per field counted in Frzb/sFRP3 transfectants (Fig. 1*D*). Compared with control cells, transfection of Frzb/sFRP3 and DN-LRP5 results in 89% and 95% inhibition of colony formation, respectively (Fig. 1*D*; Student's t test, $P < 0.01$). For anchorage-dependent growth of each transfected cell line measured by 3-(4,5-dimethylthiazol-2-yl)-2,5-diphenyltetrazolium bromide assay, Supplementary Fig. S1C showed that PC-3 cells transfected with Frzb/sFRP3 and DN-LRP5 exhibited ~1.77- and 3.57-fold higher rate of growth than PC-3 cells transfected with PCDNA3.1, respectively, after 5 days of cell seeding (growth was expressed relative to control cells where day 1 equals 100%; Student's t test, $P < 0.05$). There was no significant difference in cell growth rate between PCDNA3.1 transfectants and parental PC-3 cells (data not shown). We were also unable to detect any poly(ADP-ribose) polymerase cleavage (a hallmark for apoptosis) in any transfected cell lines, suggesting that transfections did not cause apoptosis in PC-3 cells (data not shown).

Frzb/secreted Frizzled-related protein 3 inhibits tumor growth in a xenograft mouse model. We next examined the *in vivo* effect of Frzb/sFRP3 and DN-LRP5 by inoculation of 1×10^6 PC-3 cells (transfected with Frzb/sFRP3, DN-LRP5, or PCDNA3.1) into the left flank of nude mice. Frzb/sFRP3 and DN-LRP5 transfectants initially formed small tumors, which disappeared over time. In contrast, parental PC-3 cells and PCDNA3.1 transfectants exhibited rapid tumor growth over time (each group contains 10 mice; ANOVA test, $P < 0.01$; Fig. 2). The regressed tumors from groups of Frzb/sFRP3 and DN-LRP5 transfectants did not recur during a 30-day observation period after sacrifice of the control mice.

Frzb/secreted Frizzled-related protein 3 induces expression of epithelial markers and down-regulates mesenchymal markers in PC-3 cells, suggesting a reversal of epithelial-to-mesenchymal transition. When cell morphology was examined, PC-3 cells expressing Frzb/sFRP3 were more compact and adherent to adjacent cells than PC-3 cells expressing PCDNA3.1, as seen in Fig. 3*A*. This change to a more "adhesive" cellular morphology resembles a tran-sition from a fibroblastic to an epithelial appearance. Figure 3*A* also shows that DN-LRP5 results in a similar morphology to Frzb/sFRP3 transfection.

Cells undergoing epithelial-to-mesenchymal transition are characterized by a loss of epithelial cell adhesion and cytoskeleton components and acquisition of mesenchymal components (31). We next examined the effect of Frzb/sFRP3 and DN-LRP5 transfections on the expression of epithelial marker (e.g., E-cadherin, keratin-8, and keratin-18) and mesenchymal markers (e.g., N-cadherin, vimentin, and fibronectin). Consistent with the changes in morphology, transfection of Frzb/sFRP3 and DN-LRP5 in PC-3 cells caused a dramatic induction of E-cadherin and keratin-8 and down-regulation of N-cadherin, vimentin, and fibronectin (Fig. 3*B*). P-cadherin expression was not detectable by Western blot in either control or Wnt antagonist-transfected cells (data not shown). Together, these results suggest a reversal of epithelial-to-mesenchymal transition in PC-3 cells by Frzb/sFRP3 and DN-LRP5.

The loss of E-cadherin is a hallmark of epithelial-to-mesenchymal transition (31). Transcriptional repressors, such as Slug, Snail, and Twist, have been shown to repress *E-cadherin* expression via binding to E-box motifs in the *E-cadherin* promoter (31). Among them, *Slug* has been recognized as a Wnt target gene (32), whereas Twist responded to Wnt-1 stimulation (33) and could be an activator of *N-cadherin* (34). Using real-time PCR, we showed an opposing pattern of mRNA expression for *E-cadherin* and *Slug* or

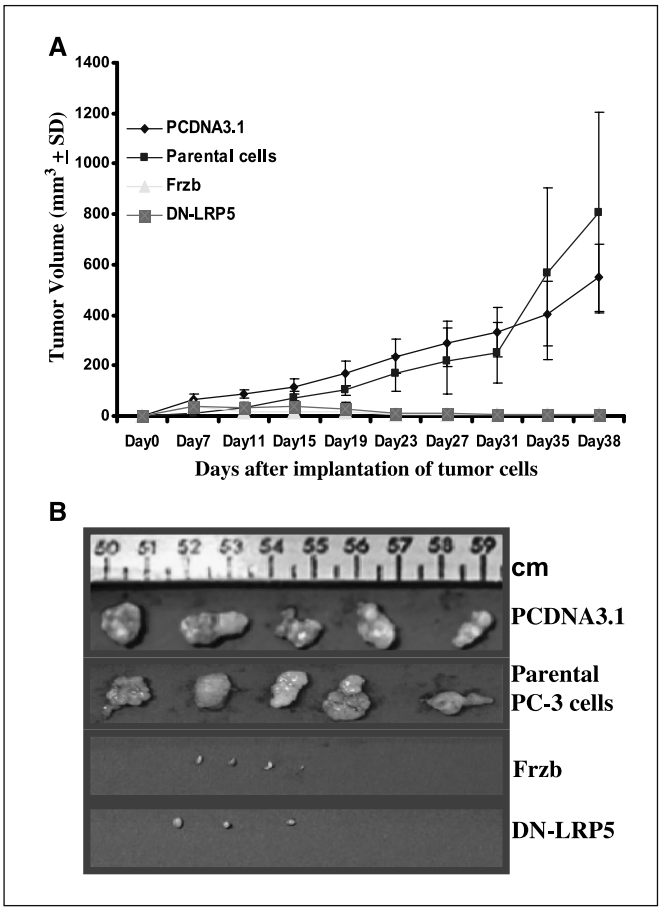

Figure 2. Expression of Frzb or DN-LRP5 results in loss of tumorigenicity of PC-3 cells in nude mice. Parental PC-3 cells or PC-3 cells transfected with PCDNA3.1 vector control, Frzb, or DN-LRP5 (2×10^6) were injected into the left flank of NCR-*nu/nu* (nude) mice. *A, points,* mean tumor volume (each group contains 10 mice); *bars,* SE. *B,* representative photograph of tumors harvested at day 38 after implantation.

Twist (Fig. 3*C*). Compared with PCDNA3.1 (Fig. 3*C*), Frzb/sFRP3 and DN-LRP5 transfectants increased *E-cadherin* expression by 23- and 12-fold but decreased *Slug* expression by 99.9% and 96.9%, respectively (Student's t test, $P < 0.01$). In addition, Frzb/sFRP3 and DN-LRP5 transfectants decreased *Twist* expression by 65% and 42% in relation to PCDNA3.1 transfectants, respectively (Student's t test, $P < 0.05$). The protein levels of Slug and Twist were also decreased in Frzb/sFRP3 and DN-LRP5 transfectants (Fig. 3*B*).

Figure 3*D* shows that intense staining of E-cadherin was observed along the entire cell-cell contact region among neighboring cells, whereas staining in the contact-free borders was weaker. These data suggest that the increased cell-cell contact seen in Frzb/sFRP3 and DN-LRP5 transfectants may be mediated by up-regulation of E-cadherin expression.

Frzb/secreted Frizzled-related protein 3 results in a decrease in invasive capacity of PC-3 cells. Based on the effects of Frzb/sFRP3 on expression of E-cadherin and N-cadherin and morphologic changes, we next examined the *in vitro* invasiveness of PC-3 cells expressing Frzb/sFRP3, DN-LRP5, DN-LEF1, DN-TCF4, or vector control in a Matrigel invasion assay. The capacity of these cells to invade through a Matrigel-coated membrane was expressed as average number of migrated cells on the lower surfaces of triplicate membranes and adjusted by

cell motility. Cell motility was measured by average number of cells migrating through a control, uncoated insert. Number of cells on each membrane was averaged from 10 fields (×100). Frzb/sFRP3-, DN-LRP5-, DN-LEF1-, and DN-TCF4-transfected cells exhibited a significant decrease in invasive capacity (by 96%, 95%, 32%, and 60%, respectively) compared with control cells (Student's t test, $P < 0.05$ to $P < 0.01$, respectively; Fig. 4).

Frzb/secreted Frizzled-related protein 3 on matrix metalloproteinase-2 and matrix metalloproteinase-9 activities and expression in PC-3 cells. Given an important role of MMP-2 and MMP-9 in prostate cancer progression and its involvement of cell-matrix interaction and tumor invasion (35–38), we examined the effect of Frzb/sFRP3 on MMP-2 and MMP-9 activities and expression. In addition, DN-LRP5, DN-TCF4, and DN-LEF1 were used to explore possible Wnt-related signaling mechanisms in regulation of MMP-2 and MMP-9. Zymography showed that ectopic expression of Frzb/sFRP3 and DN-LRP5 in PC-3 cells resulted in decreased activities of both MMP-2 (lower band) and MMP-9 (upper band) in conditioned medium (Fig. 5*A*). This decrease in MMP-2 and-9 activities correlated with lower MMP-2 and MMP-9 protein levels (Fig. 5*C* and *D*, respectively). MMP-2 and MMP-9 activities were also quantified by densitometric analysis and adjusted by total number of cells in each culture. Compared with vector control transfectants, Frzb/sFRP3, DN-LRP5, DN-LEF1, and DN-TCF4 transfectants showed a decrease in MMP-2 activity by 58%, 48%, 58%, and 30% and a decrease in MMP-9 activity by 80%, 67%, 58%, and 70% (Fig. 5*B*; Student's t test, $P < 0.05$ or $P < 0.01$).

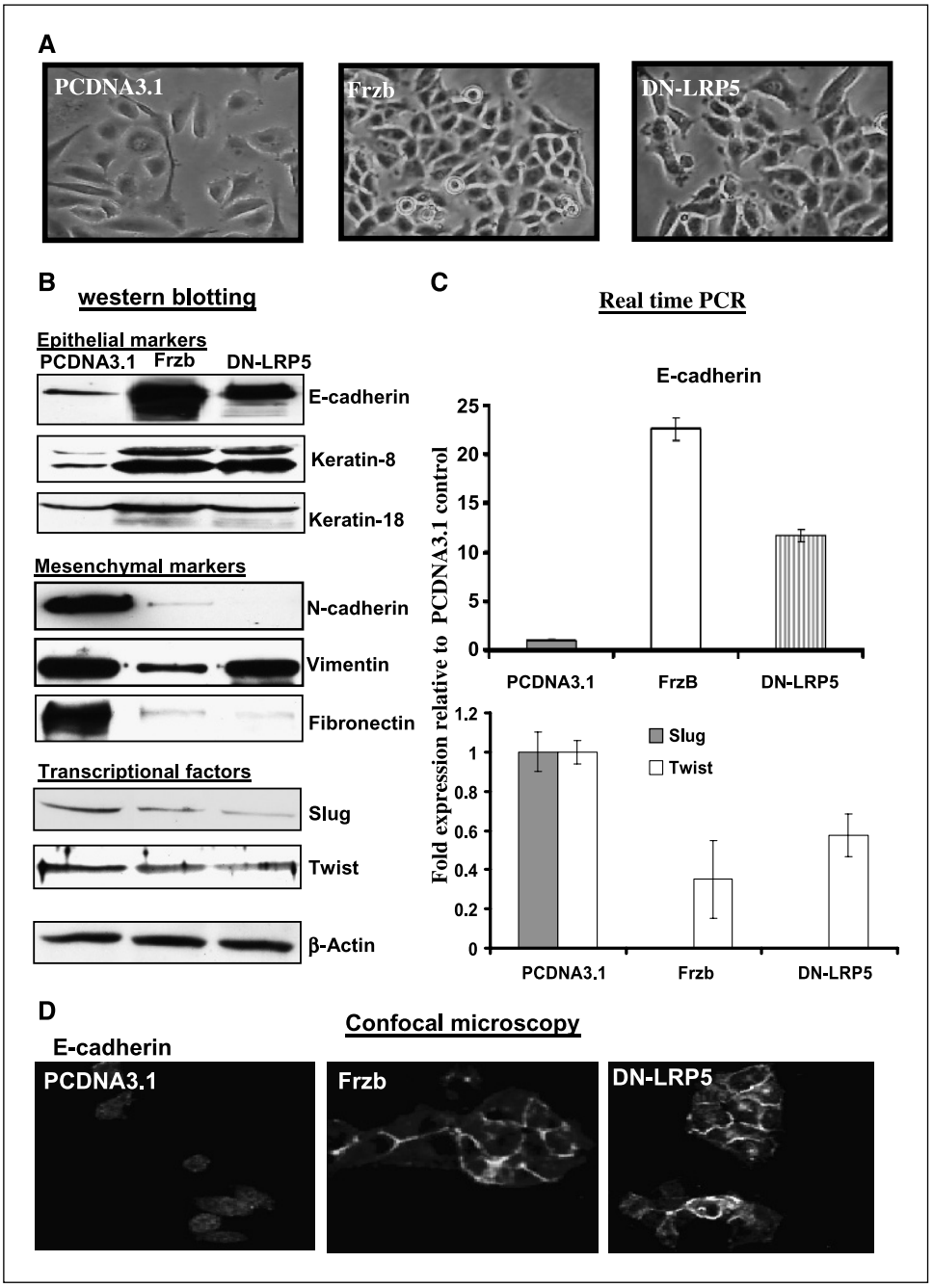

Figure 3. Ectopic expression of Frzb and DN-LRP5 is associated with changes in the profile of epithelial and mesenchymal markers and cellular morphology. *A,* representative photograph of transfected cells at 60% confluence taken under an inverted phase-contrast light microscope at ×200 magnification. *B,* Western blot analysis of expression of E-cadherin, keratin-8, keratin-18, fibronectin, N-cadherin, vimentin, Slug, Twist, and β-actin shown by a representative blot from four independent experiments. *C,* quantitative real-time PCR analysis of E-cadherin, Slug, and Twist mRNA in the transfectants. Gene expression is presented as fold increase in ΔC_t compared with PCDNA3.1 vector control transfectants. *Columns,* mean of four independent quantitative real-time PCR experiments; *bars,* SE. *D,* the transfectants were stained with anti-E-cadherin and Alex 488–conjugated secondary antibodies. Representative photograph taken under a confocal microscope (Zeiss) at ×400 magnification.

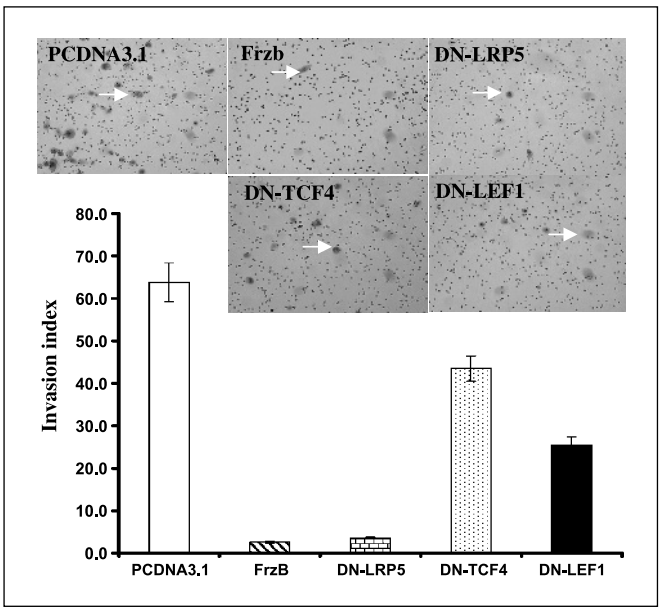

Figure 4. Expression of Frzb, DN-LRP5, DN-TCF4, or DN-LEF1 decreases the invasive capacity of PC-3 cells in a Matrigel-coated membrane. Cells were applied to the upper surface of a Matrigel-coated membrane. After incubation for 48 hours, the upper surface of the membrane was scrubbed free of cells; the membrane was fixed, stained, and photographed. Representative pictures taken from the lower surface of four independent membranes at ×100 magnification. Invasion index was calculated by adjusting cellular motility as described in detail in Materials and Methods. *Columns,* mean of invasion index calculated from four independent membranes; *bars,* SE. *Arrows,* cells that migrated through a Matrigel-coated membrane.

Effect of Frzb/secreted Frizzled-related protein 3 or dominant-negative low-density lipoprotein receptor–related protein 5 on the β-catenin/Wnt signaling pathway in PC-3 cells. Activation of the β-catenin/Wnt signaling pathway results in phosphorylation of GSK-3β and stabilization of cytosolic β-catenin leading to activation of TCF-mediated gene transcription (6). Figure 6*A* and *B* shows that expression of Frzb/sFRP3 in PC-3 cells significantly decreased the level of phospho-GSK-3β at serine-9 without affecting total GSK-3β levels. A decrease in phospho-GSK-3β represents increased activity of this protein (3). Consistently, a decrease in phospho-GSK-3β in Frzb/sFRP3 transfectants was accompanied by a decrease in cytosolic β-catenin, but the levels of membrane β-catenin were not different between Frzb/sFRP3 and control transfectants (Fig. 6*C*). To evaluate the basal levels of TCF transcriptional activities, PC-3 cells expressing PCDNA3.1, Frzb/sFRP3, or DN-LRP5 were transiently cotransfected with reporter plasmids containing either wild-type (TOPFLASH) or mutant (FOPFLASH) consensus TCF/LEF binding elements and CMV-β-galactosidase plasmids. Compared with control cells, Frzb/sFRP3 and DN-LRP5 cells exhibited decreased luciferase activities by 97.5% and 97% after adjusting for transfection efficiency in each of the cell lines (Student's t test, $P < 0.001$). There were no significant differences in c-Myc and cyclin D1 protein levels, two β-catenin/TCF4 target genes discovered in colorectal cancer cell lines, between Frzb/sFRP3 or DN-LRP5 and PCDNA3.1 transfectants (data not shown). This result is in agreement with a recent report (39) that expression of a mutant, hyperactivated form of β-catenin in some prostate cancer cell lines did not induce expression of cyclin D1 and c-myc. Together, these finding suggest that Frzb/sFRP3 or DN-LRP5 may act as a Wnt antagonist to inhibit the β-catenin/Wnt signaling pathway in PC-3 cells.

Frzb/sFRP3 and DN-LRP5, as secreted Wnt antagonists working at the membrane and extracellular levels, may affect signaling pathways besides the β-catenin/TCF4-mediated pathway. Because activation of AKT due to loss of functional phosphatase and tensin homologue is a predominant event in prostate cancer development and this activation in carcinomas leads to an invasive phenotype (40, 41), we examined the effect of Frzb/sFRP3 on AKT activation in PC-3 cells. Supplementary Fig. S2A and B shows that transfection of Frzb/sFRP3 or DN-LRP5 in PC-3 cells resulted in a significant decrease in the level of phospho-AKT but not total AKT, consistent with decreased AKT activation.

Discussion

In this study, we have characterized the tumor suppressor activity of Frzb/sFRP3 in an androgen-independent prostate cancer cellular model by showing the remarkable inhibitory effect of Frzb/sFRP3 on Matrigel invasion, colony formation, and *in vivo* tumorigenesis of PC-3 cells. We have subsequently repeated the animal experiment with a type of mesenchymal cancer. The human fibrosarcoma HT-1080 cells expressing Frzb/sFRP3 or DN-LRP5 implanted into nude mice also exhibited marked inhibition of

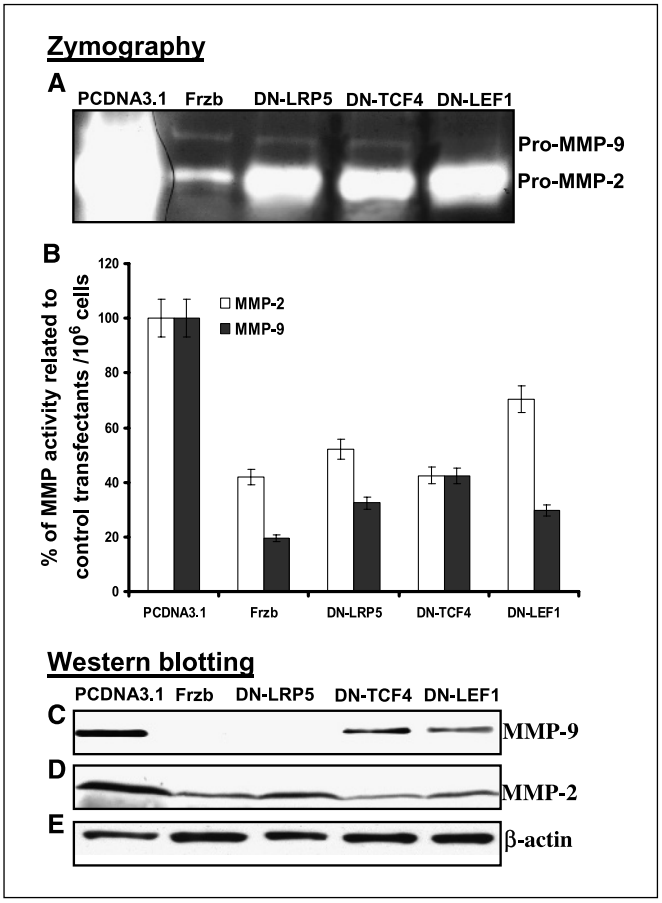

Figure 5. Expression of Frzb, DN-LRP5, DN-TCF4, or DN-LEF1 decreases MMP-2 and MMP-9 activities and their protein expression. *A,* MMP-2 and MMP-9 activities in the conditioned medium from the transfectants were assayed by zymography as described in Materials and Methods. *B,* semiquantitative comparison of MMP activities between PCDNA3.1 vector control and Frzb-, DN-LRP5-, DN-TCF4-, or DN-LEF1-transfected cells was done by densitometry. *Columns,* mean from three independent experiments; *bars,* SE. *C* to *E,* Western blot analysis of MMP-2 and MMP-9 expression. Representative blots from three independent experiments. β-Actin serves as loading control.

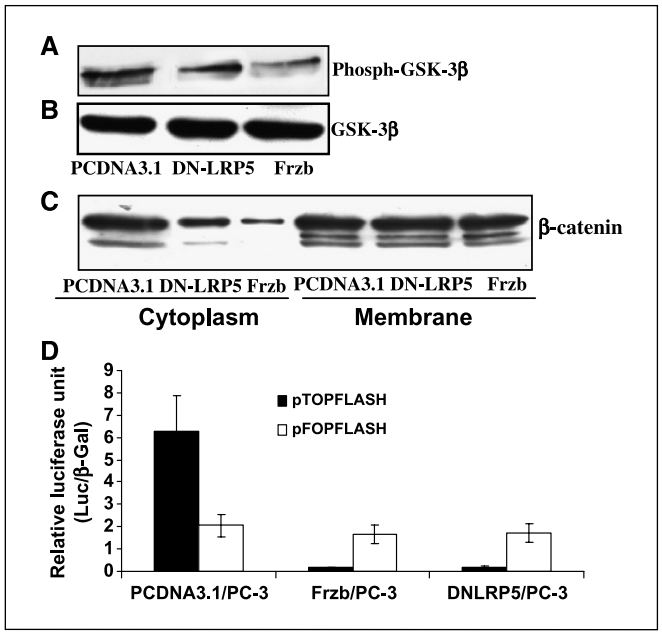

Figure 6. Changes in the Wnt signaling pathway in Frzb and DN-LRP5 transfectants. Western blot analysis was done with specific antibodies. *A,* phospho-GSK-3β. *B,* total GSK-3β. *C,* cytosolic and membrane β-catenin. *D,* PC-3 cells expressing PCDNA3.1 vector control, Frzb, and DN-LRP5 were transiently cotransfected with 1 μg pTOPFLASH or the inactive mutant pFOPFLASH and 0.1 μg pcDNA3-β-gal. After 24 hours of incubation, the cells were harvested and luciferase and β-gal activities were measured. Luciferase activity is expressed as relative luciferase unit (luciferase/β-gal). *Columns,* mean calculated from three independent experiments; *bars,* SD.

tumor growth compared with control cells.[4] This result provides further evidence for the antitumor activities of Frzb/sFRP3.

Differences in the biological effects of the various sFRPs have been reported (10–15, 42–44). In contrast to Frzb/sFRP3, FrzA/sFRP1 and sFRP2 have been shown to increase *in vivo* tumor growth of glioma cells (42). Both FrzA/sFRP1 and sFRP2 increased clonogenicity and enhanced resistance to serum starvation in glioma cell lines (42), whereas sFRP4 decreased the colony formation of glioma cells in soft agar (11). At present, it is still unclear whether differences in biological function of sFRPs reflect their specificity for various Wnt ligands and/or Frizzled receptors. The aberrantly activated Wnt signaling pathway exists in a portion of prostate cancer (2). In addition to activating mutations in the β-catenin gene (2), overexpression of Wnt-2, Wnt-5a, and Wnt-11 in prostate cancer tissues has been reported (45–47). Whether these overexpressed Wnts in prostate cancer play a role in prostatic tumorigenesis and whether Frzb/sFRP3 can actually bind to these Wnts, and thus inhibit their activities in prostate cancer cells, require further investigation.

Besides inhibiting the *in vivo* tumor formation, Frzb/sFRP3 decreased the *in vitro* invasiveness of PC-3 cells. Tumor invasiveness often correlates with increased expression of specific MMPs (35–37). We showed that both MMP-2 and MMP-9 activities can be suppressed by ectopic expression of Frzb/sFRP3 in PC-3 cells. This effect of Frzb/sFRP3 was associated with a decrease in MMP-2 and MMP-9 protein expression. These results were consistent with observation from studies of sFRP1 and sFRP2 on glioma cells (42). Structural studies of the sFRP class of Wnt antagonists revealed that these molecules contain two domains: a NH_2-terminal CRD and a COOH-terminal netrin-like domain (NTR; ref. 9). The CRD interacts with Wnt ligands and affects Wnt-mediated signaling, whereas the NTR function has not been elucidated (9). Interestingly, NTR-like domains are found in tissue inhibitors of metalloproteinases, suggesting that the NTR of sFRPs may bind to MMPs as well (9). In our study, Frzb/sFRP3 reduced expression of MMP-2 and MMP-9 proteins in PC-3 cells. The promoter regions of MMP genes (e.g., *MMP-9*) contain consensus TCF-binding region, suggesting that Frzb/sFRP3 may down-regulate MMP transcription through Wnt/TCF-mediated mechanisms (48). We further showed that transfection of a DN-TCF4, DN-LEF1, or DN-LRP5 into PC-3 cells also decreased MMP-2 and MMP-9 activities and expression. Taken together, it is tempting to speculate that the inhibitory effect of Frzb/sFRP3 on MMP-2 and MMP-9 activities may be partly dependent on its inhibition of Wnt signaling–mediated MMP expression or, in addition to possible direct binding of MMPs to Frzb/sFRP3, via the NTR domain.

In addition to increased MMP activities, acquisition of an invasive phenotype by prostate cancer may require a change in molecular profile from epithelial to mesenchymal (49). Down-regulation of E-cadherin and up-regulation of N-cadherin (the "cadherin switch"), which are consistently observed at the site of epithelial-to-mesenchymal transition during normal development and cancer, correlate with prostate cancer progression (49). Loss of E-cadherin results in dissociation of tumor cells at primary sites, whereas up-regulation of the mesenchymal-type cadherins (e.g., N-cadherin) facilitates interactions between cancer and stromal cells (31, 37, 49). In our study, expression of Frzb/sFRP3 in PC-3 cells changed cellular morphology from a fibroblastic, motile phenotype to a stationary, epithelial phenotype. These changes were accompanied by a remarkable induction of epithelial markers E-cadherin and keratin-8 as well as down-regulation of mesenchymal markers N-cadherin, fibronectin, and vimentin, resembling a reversal of epithelial-to-mesenchymal transition (31, 40). Taken together, the reversal of epithelial-to-mesenchymal transition and decreased MMP activity by Frzb/sFRP3 would indicate a less invasive tumor phenotype and thereby slow prostate cancer progression.

During most epithelial-to-mesenchymal transition situation, the Slug/Snail family and Twist, which recognize the E-box motif in the *E-cadherin* promoters, control a repressor program against epithelial phenotype (31). Interestingly, *Slug* has been identified as a Wnt target gene (32). Twist was an activator of N-cadherin in *Drosophila* embryogenesis (34) and regulated by Wnt-1. Our results showed that down-regulation of *Slug* and *Twist* mRNA and protein expressions by Frzb/sFRP3 was associated with up-regulation of E-cadherin and down-regulation of N-cadherin. Regulation of N-cadherin and E-cadherin protein levels involves differential mRNA expression, cytokine modulation, protease-mediated turnover, or phosphorylation (50). Generally, multiple pathways and their cross-talks may participate in regulating this complex cadherin switch leading to epithelial-to-mesenchymal transition and tumor invasion. Our results suggested that the reversal of epithelial-to-mesenchymal transition by Frzb/sFRP3 is involved, at least in part, both in relieving Slug- and Twist-mediated repression of *E-cadherin* transcription and in inhibiting Twist-mediated *N-cadherin* up-regulation. Further experiments using RNA interference technique are in progress to examine the role and contribution of Slug and/or Twist in the Wnt-mediated

[4] Y. Guo, X. Zi, Z. Koontz, A. Kim, J. Xie, and BH. Hoang, unpublished data.

epithelial-to-mesenchymal transition process of prostate cancer cells.

The inhibition of β-catenin-dependent Wnt signaling by expression of Frzb/sFRP3 in our study was evidenced by activation of GSK-3β and a decrease in the cytosolic β-catenin levels and TCF transcriptional activity. In addition, we observed that DN-TCF4 or DN-LRP5 shared inhibitory effects on MMP-2 and MMP-9 and on cellular invasiveness similar to Frzb/sFRP3, suggesting that these effects of Frzb/sFRP3 may be involved, at least in part, in β-catenin-dependent Wnt signaling. However, the inhibitory effect of the secreted antagonists Frzb/sFRP3 and DN-LRP5 on cellular invasiveness was more pronounced than that of DN-TCF4 and DN-LEF1 in PC-3 cells, suggesting that TCF/LEF-independent pathways are also involved in invasion. Indeed, we showed that expression of Frzb/sFRP3 in PC-3 cells significantly inhibited AKT activation. There is constitutively activated AKT in PC-3 cells due to lack of functional phosphatase and tensin homologue. Grille et al. (41) reported that overexpression of AKT in squamous cell lines resulted in epithelial-to-mesenchymal transition and increased the invasive capacity and tumorigenicity of these cell lines. Because AKT activation plays a central role in prostate cancer and AKT activation in carcinomas resulted in an invasive phenotype, further studies are needed to examine the contribution of AKT inhibition on Frzb/sFRP3-mediated effects in PC-3 cells.

In summary, our data show the tumor-suppressing activities of Frzb/sFRP3 with the marked inhibition of tumorigenicity and invasiveness of androgen-independent prostate cancer PC-3 cells. The mechanisms of the action of Frzb/sFRP3 are associated with the reversal of epithelial-to-mesenchymal transition and decreased MMP activity. The clinical relevance of our results remains to be determined in a population study. Our findings should encourage the development of Frzb/sFRP3 as a novel agent for the prevention or delay of prostate cancer progression.

Acknowledgments

Received 1/12/2005; revised 8/7/2005; accepted 8/16/2005.

Grant support: Neil Chamberlain Urological Cancer Research Fund (X. Zi and A.R. Simoneau).

The costs of publication of this article were defrayed in part by the payment of page charges. This article must therefore be hereby marked *advertisement* in accordance with 18 U.S.C. Section 1734 solely to indicate this fact.

We thank Dr. Frank P. Luyten for the *Frzb/sFRP3* construct, Dr. Matthew Warman for DN-LRP5, Dr. T.C. He for *DN-TCF4*, and Dr. Marian Waterman for the *TCF4 luciferase reporter* (TOPFLASH), a mutated control reporter (FOPFLASH), and the *LEF1* expression construct FL9B.

References

1. Bastacky SI, Wojno KJ, Walsh PC, Carmichael MJ, Epstein JI. Pathological features of hereditary prostate cancer. J Urol 1995;153:987–92.
2. Chesire DR, Ewing CM, Gage WR, Isaacs WB. *In vitro* evidence for complex modes of nuclear β-catenin signaling during prostate growth and tumorigenesis. Oncogene 2002;21:2679–94.
3. de la Taille A, Rubin MA, Chen MW, et al. β-Catenin-related anomalies in apoptosis-resistant and hormone-refractory prostate cancer cells. Clin Cancer Res 2003;9:1801–7.
4. Amir AL, Barua M, McKnight NC, et al. direct β-catenin-independent interaction between androgen receptor and T cell factor 4. J Biol Chem 2003;278:30828–34.
5. Truica CI, Byers S, Gelmann EP. β-Catenin affects androgen receptor transcriptional activity and ligand specificity. Cancer Res 2000;60:4709–13.
6. Moon RT, Kohn AD, De Ferrari GV, Kaykas A. WNT and β-catenin signaling: diseases and therapies. Nat Rev Genet 2004;5:691–701.
7. Nelson WJ, Nusse R. Convergence of Wnt, β-catenin, and cadherin pathways. Science 2004;303:1483–7.
8. Veeman MT, Axelrod JD, Moon RT. A second canon. Functions and mechanisms of β-catenin-independent Wnt signaling. Dev Cell 2003;5:367–77.
9. Kawano Y, Kypta R. Secreted antagonists of the Wnt signaling pathway. J Cell Sci 2003;116:2627–34.
10. Suzuki H, Watkins DN, Jair KW, et al. Epigenetic inactivation of SFRP genes allows constitutive WNT signaling in colorectal cancer. Nat Genet 2004;36:417–22.
11. Lee AY, He B, You L, et al. Expression of the secreted frizzled-related protein gene family is downregulated in human mesothelioma. Oncogene 2004;23:6672–6.
12. Klopocki E, Kristiansen G, Wild PJ, et al. Loss of SFRP1 is associated with breast cancer progression and poor prognosis in early stage tumors. Int J Oncol 2004;25:641–9.
13. Stoehr R, Wissmann C, Suzuki H, et al. Deletions of chromosome 8p and loss of sFRP1 expression are progression markers of papillary bladder cancer. Lab Invest 2004;84:465–78.
14. Suzuki H, Gabrielson E, Chen W, et al. A genomic screen for genes upregulated by demethylation and histone deacetylase inhibition in human colorectal cancer. Nat Genet 2002;31:141–9.
15. Ugolini F, Charafe-Jauffret E, Bardou VJ, et al. WNT pathway and mammary carcinogenesis: loss of expression of candidate tumor suppressor gene SFRP1 in most invasive carcinomas except of the medullary type. Oncogene 2001;20:5810–7.
16. Hoang B, Moos M, Jr., Vukicevic S, Luyten FP. Primary structure and tissue distribution of FRZB/SFRP3, a novel protein related to *Drosophila* frizzled, suggest a role in skeletal morphogenesis. J Biol Chem 1996;271:26131–7.
17. Wang S, Krinks M, Lin K, Luyten FP, Moos M, Jr. Frzb, a secreted protein expressed in the Spemann organizer, binds and inhibits Wnt-8. Cell 1997;88:757–66.
18. Leyns L, Bouwmeester T, Kim SH, Piccolo S, De Robertis EM. Frzb-1 is a secreted antagonist of Wnt signaling expressed in the Spemann organizer. Cell 1997;88:747–56.
19. Peichel CL, Kozak CA, Luyten FP, Vogt TF. Evaluation of mouse Sfrp3/Frzb1 as a candidate for the lst, Ul, and Far mutants on chromosome 2. Mamm Genome 1998;9:385–7.
20. Wolf M, Mousses S, Hautaniemi S, et al. High-resolution analysis of gene copy number alterations in human prostate cancer using CGH on cDNA microarrays: impact of copy number on gene expression. Neoplasia 2004;6:240–7.
21. Schmitt JF, Millar DS, Pedersen JS, et al. Hypermethylation of the inhibin α-subunit gene in prostate carcinoma. Mol Endocrinol 2002;16:213–20.
22. Nishizuka S, Tamura G, Terashima M, Satodate R. Loss of heterozygosity during the development and progression of differentiated adenocarcinoma of the stomach. J Pathol 1998;185:38–43.
23. Simon R, Burger H, Brinkschmidt C, et al. Chromosomal aberrations associated with invasion in papillary superficial bladder cancer. J Pathol 1998;185:345–51.
24. Shiseki M, Kohno T, Nishikawa R, et al. Frequent allelic losses on chromosomes 2q, 18q, and 22q in advanced non-small cell lung carcinoma. Cancer Res 1992;52:2478–81.
25. Ransom DT, Barnett TC, Bot J, et al. Loss of heterozygosity on chromosome 2q: possibly a poor prognostic factor in head and neck cancer. Head Neck 1998;20:404–10.
26. Gong Y, Slee RB, Fukai N, et al. Osteoporosis-Pseudoglioma Syndrome Collaborative Group. LDL receptor-related protein 5 (LRP5) affects bone accrual and eye development. Cell 2001;107:513–23.
27. He TC, Sparks AB, Rago C, et al. Identification of c-MYC as a target of the APC pathway. Science 1998;281:1509–12.
28. Shimizu H, Julius MA, Giarre M, et al. Transformation by Wnt family proteins correlates with regulation of β-catenin. Cell Growth Differ 1997;8:1349–58.
29. Tsai CN, Tsai CL, Tse KP, Chang HY, Chang YS. The Epstein-Barr virus oncogene product, latent membrane protein 1, induces the downregulation of E-cadherin gene expression via activation of DNA methyltransferases. Proc Natl Acad Sci U S A 2002;99:10084–9.
30. Dhanasekaran SM, Barrette TR, Ghosh D, et al. Delineation of prognostic biomarkers in prostate cancer. Nature 2001;412:822–6.
31. Kang Y, Massague J. Epithelial-mesenchymal transitions: twist in development and metastasis. Cell 2004;118:277–9.
32. Vallin J, Thuret R, Giacomello E, et al. Cloning and characterization of three *Xenopus* Slug promoters reveal direct regulation by Lef/β-catenin signaling. J Biol Chem 2001;276:30350–8.
33. Howe LR, Watanabe O, Leonard J, Brown AM. Twist is up-regulated in response to Wnt1 and inhibits mouse mammary cell differentiation. Cancer Res 2003;63:1906–13.
34. Oda H, Tsukita S, Takeichi M. Dynamic behavior of the cadherin-based cell-cell adhesion system during *Drosophila* gastrulation. Dev Biol 1998;203:435–50.
35. Luo J, Lubaroff DM, Hendrix MJ. Suppression of prostate cancer invasive potential and matrix metalloproteinase activity by E-cadherin transfection. Cancer Res 1999;59:3552–6.
36. Kuniyasu H, Ukai R, Johnston D, et al. The relative mRNA expression levels of matrix metalloproteinase to E-cadherin in prostate biopsy specimens distinguishes organ-confined from advanced prostate cancer at radical prostatectomy. Clin Cancer Res 2003;9:2185–94.
37. Nagle RB, Knox JD, Wolf C, Bowden GT, Cress AE. Adhesion molecules, extracellular matrix, and proteases in prostate carcinoma. J Cell Biochem Suppl 1994;19:232–7.
38. Zhao YG, Xiao AZ, Newcomer RG, et al. Activation of pro-gelatinase B by endometase/matrilysin-2 promotes invasion of human prostate cancer cells. J Biol Chem 2003;278:15056–64.

39. Chesire DR, Dunn TA, Ewing CM, Luo J, Isaacs WB. Identification of aryl hydrocarbon receptor as a putative Wnt/β-catenin pathway target gene in prostate cancer cells. Cancer Res 2004;64:2523–33.

40. Kreisberg JI, Malik SN, Prihoda TJ, et al. Phosphorylation of Akt (Ser^{473}) is an excellent predictor of poor clinical outcome in prostate cancer. Cancer Res 2004;64:5232–6.

41. Grille SJ, Bellacosa A, Upson J, et al. The protein kinase Akt induces epithelial mesenchymal transition and promotes enhanced motility and invasiveness of squamous cell carcinoma lines. Cancer Res 2003;63:2172–8.

42. Roth W, Wild-Bode C, Platten M, et al. Secreted Frizzled-related proteins inhibit motility and promote growth of human malignant glioma cells. Oncogene 2000; 19:4210–20.

43. Melkonyan HS, Chang WC, Shapiro JP, et al. SARPs: a family of secreted apoptosis-related proteins. Proc Natl Acad Sci U S A 1997;94:13636–41.

44. Horvath LG, Henshall SM, Kench JG, et al. Membranous expression of secreted frizzled-related protein 4 predicts for good prognosis in localized prostate cancer and inhibits PC3 cellular proliferation *in vitro*. Clin Cancer Res 2004;10:615–25.

45. Katoh M. Frequent up-regulation of WNT2 in primary gastric cancer and colorectal cancer. Int J Oncol 2001;19:1003–7.

46. Iozzo RV, Eichstetter I, Danielson KG. Aberrant expression of the growth factor Wnt-5A in human malignancy. Cancer Res 1995;55:3495–99.

47. Zhu H, Mazor M, Kawano Y, et al. Analysis of Wnt gene expression in prostate cancer: mutual inhibition by WNT11 and the androgen receptor. Cancer Res 2004;64: 7918–26.

48. Marchenko GN, Marchenko ND, Leng J, Strongin AY. Promoter characterization of the novel human matrix metalloproteinase-26 gene: regulation by the T-cell factor-4 implies specific expression of the gene in cancer cells of epithelial origin. Biochem J 2002;363: 253–62.

49. Hazan RB, Qiao R, Keren R, Badano I, Suyama K. Cadherin switch in tumor progression. Ann N Y Acad Sci 2004;1014:155–63.

50. Lee MM, Fink BD, Grunwald GB. Evidence that tyrosine phosphorylation regulates N-cadherin turnover during retinal development. Dev Genet 1997;20:224–34.

Expression of Frzb/Secreted Frizzled-Related Protein 3, a Secreted Wnt Antagonist, in Human Androgen-Independent Prostate Cancer PC-3 Cells Suppresses Tumor Growth and Cellular Invasiveness

Xiaolin Zi, Yi Guo, Anne R. Simoneau, et al.

Cancer Res 2005;65:9762-9770.